

# Optimization, and Evaluation of Hyaluronic Acid Conjugated PLGA Nanoparticles of Etoposide for Cancer Treatment

Bhakti Patil, Prakash Kumar Soni, Suresh Kumar Paswan

Department of Pharmacy, Shri G.S Institute Technology and Science, Indore, Madhya Pradesh, India

## Abstract

**Introduction:** Etoposide is used for the treatment of small-lung cancer. It is associated with the major side effect of secondary leukemia. Targeting of formulation subdues the side effects associated with etoposide making it safer for use. The current work aims to prepare and evaluate etoposide-loaded poly (lactic-co-glycolic acid)-polyethylene glycol hyaluronic acid (PLGA-PEG-HA) nanoparticles to deliver etoposide to lung cancer cells by active targeting of the CD44 receptor. **Materials and Methods:** Nanoparticles were prepared using the emulsification solvent evaporation technique and Box-Behnken design was employed to optimize the formulation, and the effect of independent variables, that is, PLGA-PEG-HA, Polyvinyl alcohol solution, etoposide on formulation was analyzed. Scanning electron microscopy, differential scanning calorimetry, X-ray diffraction, and *in vitro* drug release studies were used to evaluate etoposide-loaded PLGA-PEG-HA nanoparticles. The cytotoxicity of the formulation on the A549 cell line was to evaluate the mortality rate of cancer cells. **Results and Discussion:** The average particle size, poly-dispersibility index, zeta potential, and entrapment efficiency were 283.35 nm, 0.57,  $-8.70$  nm, and 53.21%, respectively. The optimized batch showed 10.69% immediate release and 6 h sustained release and the drug release pattern followed the Korsmeyer-Peppas model. In the cell line study, the formulation showed a cell mortality rate of 72.14% and an  $IC_{50}$  value of  $2 \mu M$ . **Conclusion:** Etoposide-loaded PLGA-PEG-HA nanoparticles for targeted delivery of etoposide to lung cancer cells were successfully prepared. The results showed that etoposide-loaded PLGA-PEG-HA nanoparticles have significantly increased cell death at concentrations considerably lower than those of free etoposide. It will reduce the overall dose required and improve the safety of treatment, which could ultimately lead to better outcomes for patients.

**Key words:** Box-Behnken design, emulsification solvent evaporation, etoposide, lung cancer, probe sonication, targeted nanoparticle

## INTRODUCTION

Lung cancer is the most common cancer and it is the main cause of death in both genders.<sup>[1]</sup> It has a high degree of invasiveness and spreads quickly. It shows various symptoms depending upon the site in the bronchi.<sup>[2]</sup> Small cell lung cancer (SCLC) spreads more quickly than other types of lung cancer due to its rapid cell division.<sup>[3]</sup> Etoposide is a semisynthetic podophyllum derivative that is pharmacologically active against various malignancies including small-cell lung carcinoma.<sup>[4]</sup> It works by blocking an enzyme topoisomerase II, which helps to untangle and organize DNA in cells by cutting and repairing the bonds between the two strands of DNA. This process is important for many processes in cells, including replication and transcription.<sup>[5]</sup> However, if the DNA damage caused by etoposide is not properly repaired,

it can lead to secondary leukemia.<sup>[6]</sup> At present, the only available forms of etoposide are injectables and capsules, which do not have targeted action and may cause side effects.<sup>[7]</sup> Nanoparticles have the potential to be used for targeted drug delivery in cancer treatment because they can penetrate cell membranes, bind to specific proteins, and escape from the lysosome following endocytosis. These abilities can help minimize the side effects associated with traditional dosage forms.<sup>[8,9]</sup> Poly (lactic-co-glycolic acid) (PLGA) nanoparticles are often used for this purpose because they are biodegradable and biocompatible.<sup>[10]</sup> To achieve site-selective delivery, nanoparticles can be equipped with

### Address for correspondence:

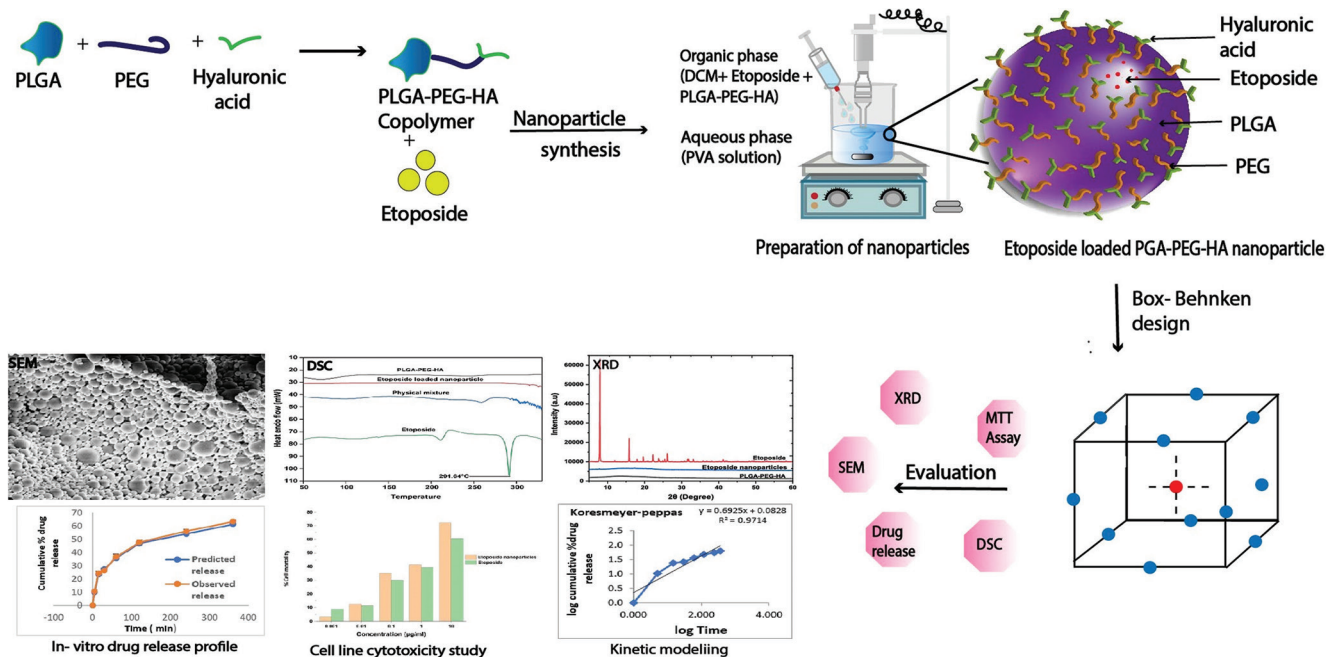
Suresh Kumar Paswan, Department of Pharmacy, Shri G.S Institute Technology and Science, Indore, Madhya Pradesh, India. E-mail: skpaswan@gmail.com

**Received:** 02-01-2023

**Revised:** 04-03-2023

**Accepted:** 14-03-2023

## GRAPHICAL ABSTRACT



recognition ligands that bind to specific receptors at the target site.<sup>[11]</sup> Cancer cells often overexpress certain receptors, such as the CD44 receptor, which can be targeted using these ligands.<sup>[12,13]</sup> Hyaluronic acid (HA) is a promising choice among ligands for active targeting in lung cancer treatment because it is biodegradable and can specifically bind to CD44 receptors.<sup>[14,15]</sup>

The present study aims to prepare etoposide-loaded PLGA-polyethylene glycol-HA (PLGA-PEG-HA) nanoparticles that can be used to deliver etoposide to tumor cells in a targeted and sustained manner. Surface modification of PLGA is done with HA as a ligand using diamino PEG as a linker. HA has a specific affinity for the CD44 receptor, which is often overexpressed on the surface of cancer cells. The nanoparticles are designed to be taken up by tumor cells through receptor-mediated uptake. The nanoparticles will specifically target the tumor cells and will release the drug over a longer period, potentially leading to more effective treatment and fewer side effects.

## EXPERIMENT

### Materials and methods

Etoposide and PLGA 50:50 (Purasorb PDLG 5002 intrinsic viscosity 0.2 dl/g, MW 75,000 Da) were procured as a gift sample from M/s Zydus Research Center, Ahmedabad, India, and M/s Biochem, respectively. PEG bis-amine (3,400 Da), Sodium hyaluronate (800,000–1,000,000 Da) Polyvinyl alcohol (PVA, 86.5% hydrolyzed, MW 1,60,00 Da), N-hydroxy-succinimide

(NHS), (1-Ethyl-3-(3-dimethyl aminopropyl) carbodiimide (EDAC), N, N'-dicyclohexylcarbodiimide (DCC) purchased from Thermofisher India, CosChemSupply, HI Media, Avra, Spectrochem, respectively.

### Synthesis of PLGA-PEG-HA copolymer

The PLGA-PEG-HA copolymer was synthesized in a series of steps which included activation of PLGA, coupling of activated PLGA to form PLGA-PEG-NH<sub>2</sub>, further the activation of ligand was performed followed by attachment of ligand. The activation of PLGA was done by dissolving a weighed amount of PLGA (2.00 g) in 30 mL of methylene chloride, NHS (11.50 mg), and DCC (20.66 mg) were added into the reaction flask and the reaction was carried out in a nitrogen atmosphere for 24 h at room temperature. The resultant solution was filtered through Whatman filter paper to remove urea crystals formed. To the solution containing activated PLGA (PLGA-NHS), di-amino-PEG (136.00 mg) was added and a coupling reaction was carried out in a nitrogen environment for 24 h at room temperature. The excess solvent of the reaction mixture was evaporated by the rotatory evaporator and the residue (PLGA-PEG-NH<sub>2</sub>) obtained was dissolved in 10 mL acetone. Simultaneously in a separate reaction flask, sodium hyaluronate (29.96 mg) and EDAC (2.47 mg) were dissolved in 200 mL of Milli-Q water and stirred for 12 h. The PLGA-PEG-NH<sub>2</sub> dissolved in acetone was added dropwise into activated HA and the reaction was carried out for 48 h at room temperature. PLGA-PEG-HA was collected by centrifuging the reaction mixture at 5000 rpm for 15 min.<sup>[16]</sup>

## Formulation of etoposide-loaded PLGA-PEG-HA nanoparticle

Etoposide-loaded nanoparticles were formulated by emulsification solvent evaporation technique. Etoposide (5–10 mg) and PLGA-PEG-HA copolymer (90–100 mg) were dissolved in 5 mL of methylene chloride as an organic phase and added dropwise to the aqueous solution of 100 mL PVA (0.2–0.5%) with probe sonicating for 3 min to form the primary emulsion. Further, the emulsion was stirred overnight to evaporate methylene chloride, centrifuged at 5000 rpm, and washed thrice with milli-Q water to remove PVA and collect the nanoparticles. The nanoparticles were freeze-dried with 5% mannitol and stored at  $-20^{\circ}\text{C}$  in the refrigerator for further use.<sup>[17,18]</sup>

## Experimental approach

The optimization was carried out to reduce the number of experimental trials. Etoposide-loaded PLGA-PEG-HA nanoparticles were formulated by emulsification solvent evaporation technique. In the present study, the Box-Behnken design (BBD) was selected to evaluate the effect of independent variables. The independent variables selected were etoposide concentration (A), PLGA-PEG-HA copolymer concentration (B), and PVA concentration (C). The evaluation of prepared nanoparticles was done by dependent variables, that is, particle size (R1), poly-dispersibility index (PDI) (R2), zeta potential (R3), entrapment efficiency (R4), and cumulative % drug release:

5 min (R5), 15 min (R6), 30 min (R7), 60 min (R8), 120 min (R9), 240 min (R10), and 360 min (R11). The dependent and independent variables and their levels are represented in Table 1. The optimization batches given by the software is shown in Table 2.

The experimental data were analyzed to examine the relationship between the independent variables and the dependent variable using Design Expert® software (version 12, stat-Ease, Inc., Minneapolis, MN). The BBD was employed and the software suggested 15 batches. Analysis of variance was used to determine the statistical significance of the model, with a *P*-value threshold of 0.05. The appropriateness was estimated by the coefficient of correlation ( $R^2$ ) and adjusted  $R^2$ . The optimized formulation was then prepared and compared to the predicted value.

## EVALUATION OF ETOPOSIDE-LOADED PLGA-PEG-HA NANOPARTICLES

### Particle size and PDI determination and zeta potential

The average particle size and poly-dispersity index of the optimization batches of etoposide-loaded PLGA-PEG-HA nanoparticles were determined using a particle size analyzer (Horiba SZ 100). The principle involved in particle size analysis

**Table 1: Variables and their levels**

Independent variables				
Components	Unit	Level		
		Low	Medium	High
A: Etoposide	mg	5	7.5	10
B: PLGA-PEG-HA copolymer	mg	90	95	100
C: PVA	%	0.2	0.35	0.5
Dependent variables				
Responses	Unit	Level		
Particle size (R1)	nm	Minimum		
PDI (R2)	-	Minimum		
Zeta potential (R3)	mV	Maximum		
Entrapment efficiency (R4)	%	Maximum		
Cumulative % drug release in 5 min (R5)	%	Minimum		
Cumulative % drug release in 15 min (R6)	%	Minimum		
Cumulative % drug release in 30 min (R7)	%	Minimum		
Cumulative % drug release in 60 min (R8)	%	Minimum		
Cumulative % drug release in 120 min (R9)	%	Minimum		
Cumulative % drug release in 240 min (R10)	%	Minimum		
Cumulative % drug release in 360 min (R11)	%	Minimum		

PLGA-PEG-HA: Poly (lactic-co-glycolic acid)-polyethylene glycol hyaluronic acid, PVA: Polyvinyl alcohol

**Table 2:** Independent variables of Box-Behnken design

Independent variable	Optimization batches														
	1	2	3	4	5	6	7	8	9	10	11	12	13	14	15
PLGA-PEG-HA copolymer (mg)	5.0	5.0	10	10	7.5	7.5	7.5	7.5	5.0	10	5.0	10	7.5	7.5	7.5
Etoposide (mg)	90	100	90	100	90	100	90	100	95	95	95	95	95	95	95
Surfactant (mg)	0.35	0.35	0.35	0.35	0.20	0.20	0.50	0.50	0.20	0.20	0.50	0.50	0.35	0.35	0.35

PLGA-PEG-HA: Poly (lactic-co-glycolic acid)-polyethylene glycol hyaluronic acid

**Table 3:** Regression equations for the response variable

Response variable	Polynomial equation
Particle size (R1)	$243.40+6.21A-2.97B-53.06C-7AB+1.92AC-5.85BC-14.96A^2+53.11B^2+36.74C^2$
PDI (R2)	$0.2187+0.0711A+0.0740B+0.0119C-0.0898AB+0.2010AC+0.0468BC-0.0061A^2+0.2282B^2+0.2309C^2$
Zeta potential (R3)	$-16.67+0.8125A+3.91B+1.60C+5.10AB-3.52AC+2.17BC+0.3583A^2+0.6083B^2+5.98C^2$
Entrapment Efficiency (R4)	$37.33+11.07A-0.3263B-3.52C-4.87AB-6.26AC-1.87BC-2.02A^2+11.70B^2+4.09C^2$
Cumulative % drug release in 5 min (R5)	$22.82-6.80A+1.63B-1.01C-4.72AB-1.61AC-0.2996BC-8.05A^2-3.31B^2+6.09C^2$
Cumulative % drug release in 15 min (R6)	$37.84-4.61A-0.4126B+1.08C-0.6892AB-1.92AC-1.43BC-7.65A^2-7B^2+3.87C^2$
Cumulative % drug release in 30 min (R7)	$40.12-3.44A-1.23B-0.0119C-1.73AB-0.0692AC-1.20BC-2.36A^2-7.09B^2+4.56C^2$
Cumulative % drug release in 60 min (R8)	$41.87-1.26A-2.33B-0.0870C+0.1491AB+3.76AC-3.35BC+2.43A^2-4.41B^2+5.09C^2$
Cumulative % drug release in 120 min (R9)	$44.24+0.9186A-1.59B-0.7727C+2.80AB+9.25AC-2.45BC+8.07A^2-2.28B^2+6.95C^2$
Cumulative % drug release in 240 min (R10)	$47.24+1.85A-3.07B+0.1130C+4.02AB+13.57AC-4.48BC+9.91A^2+0.8021B^2+9.29C^2$
Cumulative % drug release in 360 min (R11)	$51.90+0.3128A-2.42B-2.09C+5.81AB+13.98AC-5.22BC+11.02A^2+2.58B^2+11.62C^2$

was dynamic light scattering. The nanoparticle suspension was placed in a glass cuvette and analyzed using milli-Q water as the dispersion medium to suspend the nanoparticles.<sup>[19]</sup> The zeta potential of the optimization batches of etoposide-loaded PLGA-PEG-HA nanoparticles was determined using a zeta potential analyzer (Horiba SZ 100). The principle involved in zeta potential analysis was laser Doppler electrophoresis. The dilute nanoparticles suspension was placed in a glass cuvette and analyzed at 25°C with an electrode voltage of 3.8 V. Particles suspended in a liquid will undergo motion due to the presence of an electric field. The charge on the surface of these particles can be determined by analyzing their movement in the field.<sup>[20]</sup> The experimental observations of the optimization batches and optimized batch are recorded in Tables 4 and 6, respectively, and graphically represented in Figure 27.

### Entrapment efficiency

The entrapment of etoposide within the polymer matrix of the nanoparticle is determined. Etoposide-loaded nanoparticles equivalent to 10 mg were taken in 2 mL of methylene chloride

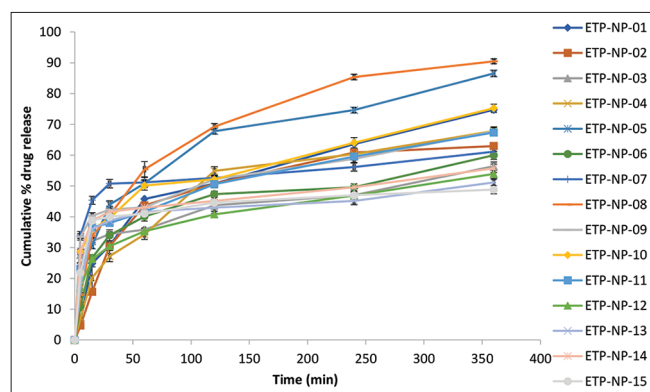


**Figure 1:** Drug release profile of optimization batches of etoposide-loaded poly (lactic-co-glycolic acid)-polyethylene glycol hyaluronic acid nanoparticles. Values shown in the graph are recorded as mean  $\pm$  standard deviation, where  $n = 3$ , error bar indicates the standard deviation of replicates

and sonicated for 10 min to dissolve the PLGA-PEG-HA further 8 mL of ethanol was added, and the resultant mix was sonicated once again for 10 min to dissolve etoposide. The mixture was centrifuged and the supernatant was collected

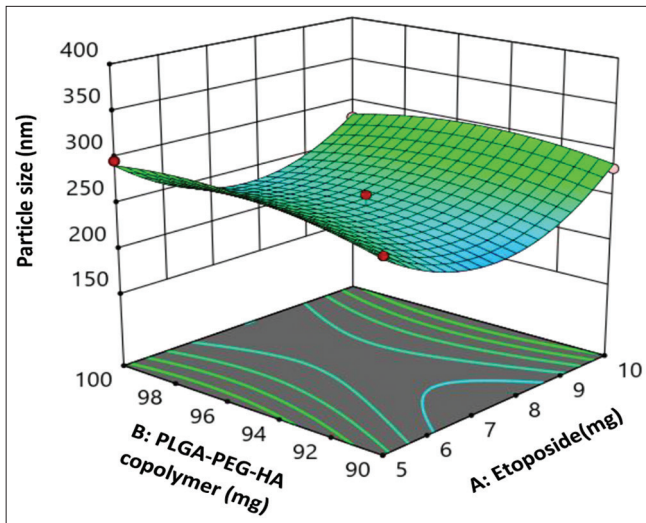


**Figure 2:** 3-D plot of the effect of etoposide and poly (lactic-co-glycolic acid)-polyethylene glycol hyaluronic acid copolymer on particle size

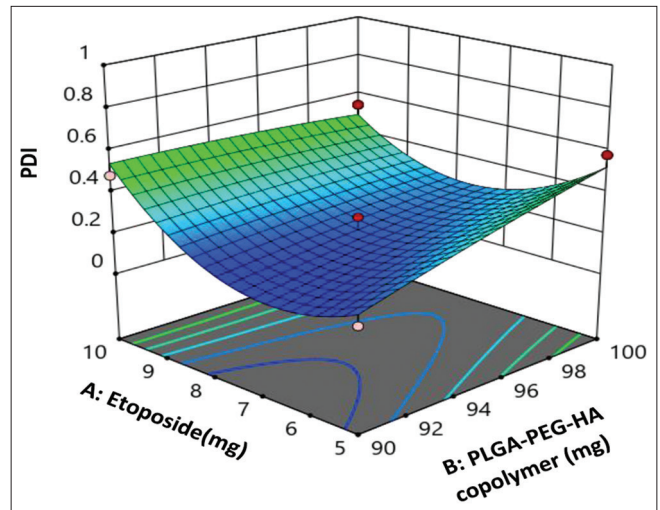


**Figure 4:** 3-D plot of the effect of etoposide and poly (lactic-co-glycolic acid)-polyethylene glycol hyaluronic acid copolymer on PDI

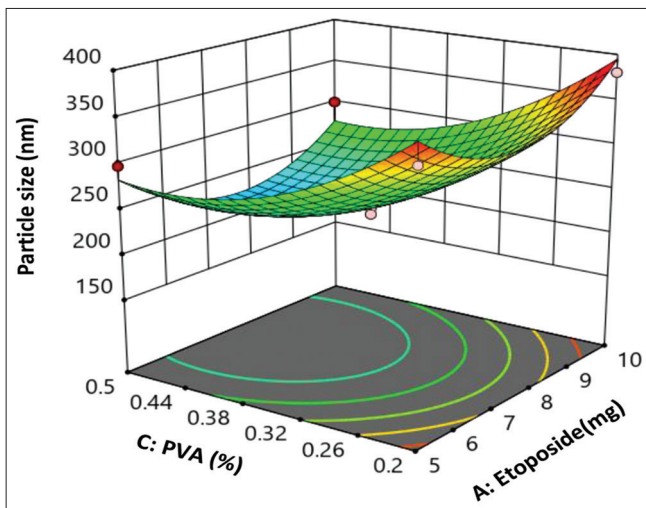


**Figure 3:** 3-D plot of the effect of polyvinyl alcohol and etoposide on particle size

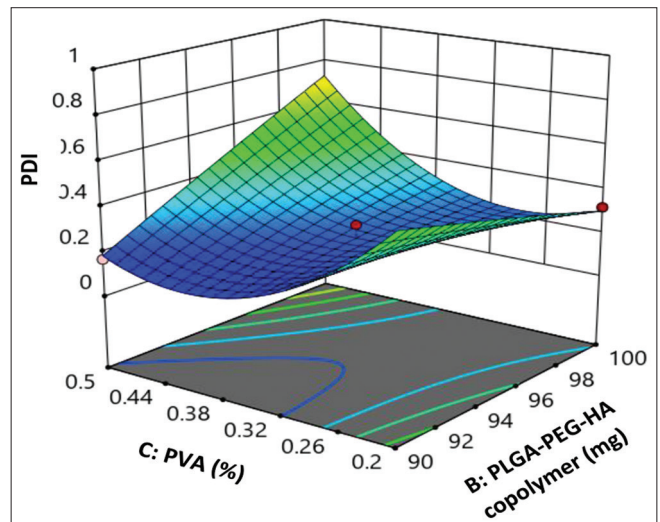


**Figure 5:** 3-D plot of the effect of polyvinyl alcohol and poly (lactic-co-glycolic acid)-polyethylene glycol hyaluronic acid copolymer on PDI

and analyzed through a UV spectrophotometer (Shimadzu 1700) at 283 nm

$$\% \text{ Entrapment efficiency} = \frac{\text{Practical observed drug loading}}{\text{Theoretical drug loading}} * 100$$

The entrapment efficiency of the optimization batches and the optimized batch is recorded in Tables 4 and 6, respectively.

### Scanning electron microscopy (SEM)

Field-emission electron microscopy (Supra 55 Zeiss) FE-SEM was used to analyze the morphology of the

etoposide nanoparticle. A small quantity of lyophilized etoposide-loaded PLGA-PEG-HA nanoparticles was placed on an aluminum stub with the help of double-sided carbon tape and subjected to gold vapors to coat the samples and then observed under FE-SEM at 5 kV. The microscopic image of FE-SEM is shown in Figure 28.

### Differential scanning calorimetry (DSC)

The polymorphic nature of the materials was analyzed through DSC. The thermal behavior of PLGA-PEG-HA copolymer, physical mixture, etoposide, and etoposide-loaded PLGA-PEG-HA nanoparticles were analyzed on DSC-6000 (PerkinElmer Thermal Analysis). The

Table 4: Dependent variables in Box-Behnken design of PLGA-PEG-HA nanoparticles

S.No.	Response variables										
	R1: Average particle size (nm)	R2: PDI	R3: Zeta potential (mV)	R4: Entrapment efficiency (%)	R5: 5 min	R6: 15 min	R7: 30 min	R8: 60 min	R9: 120 min	R10: 240 min	R11: 360 min
1	268.7±0.24	0.160	-18.7	27.5±0.65	6.27±0.54	24.86±0.91	30.65±1.24	45.76±0.97	50.76±0.53	63.58±0.80	74.74±1.77
2	296.7±0.67	0.580	-22.3	63.7±0.34	4.72±0.54	15.67±0.86	30.46±0.69	43.67±0.60	50.76±1.20	60.84±1.11	62.97±0.47
3	280.4±0.87	0.481	-19.3	40.0±0.64	27.63±1.01	32.09±1.19	34.34±0.80	35.80±0.54	43.69±1.97	47.00±1.9	56.40±1.37
4	280.4±1.23	0.542	-2.5	57.0±0.24	7.20±0.81	20.14±1.35	27.22±1.78	34.30±1.67	54.89±1.33	60.35±0.95	67.86±1.33
5	333.7±0.54	0.676	-13.9	27.3±0.78	23.87±1.31	30.61±0.95	43.96±1.23	50.85±1.13	67.79±0.89	74.64±0.88	86.54±1.04
6	340.7±0.65	0.318	-10.2	57.3±1.61	10.88±1.33	26.61±1.12	34.01±1.74	40.10±1.497	47.36±0.95	49.58±1.07	60.00±1.33
7	185.8±0.93	0.167	-3.4	34.0±0.45	34.06±1.11	45.37±1.30	50.77±1.36	51.15±1.58	52.65±0.90	56.14±1.32	61.11±0.97
8	200.5±0.56	0.613	-13.8	39.0±0.16	14.65±0.71	33.67±1.06	40.54±0.95	55.42±2.45	69.23±1.06	85.36±0.90	90.47±0.80
9	354.4±0.78	0.570	-12.4	57.5±0.67	33.49±1.04	40.33±0.99	42.31±1.09	43.09±1.09	52.14±1.1	58.82±1.18	67.79±1.25
10	380.3±1.76	0.631	-10.7	57.0±0.34	28.70±1.07	35.69±0.66	39.58±0.81	50.15±1.48	52.14±0.99	64.03±1.67	75.27±1.30
11	297.9±0.89	0.631	-13.8	53.0±0.78	23.09±1.95	36.59±1.03	38.00±0.84	41.64±1.17	50.59±1.20	59.58±1.14	67.36±1.16
12	300.4±0.36	0.879	-3.4	45.0±0.17	17.10±1.66	26.24±0.79	30.46±1.40	35.29±1.01	40.78±0.99	46.89±1.08	53.96±1.50
13	240.9±0.56	0.28	-22.5	42.0±0.81	17.81±1.26	36.00±1.55	38.76±0.79	41.59±1.04	42.99±1.81	45.13±1.25	51.15±0.99
14	255.7±0.16	0.171	-13.7	37.0±1.47	28.81±0.56	38.76±0.90	41.59±1.05	42.99±0.99	45.13±1.07	49.58±1.12	55.74±1.39
15	233.6±0.45	0.205	-13.8	33.0±0.37	21.81±0.92	38.76±0.59	40.00±1.72	41.01±0.07	44.59±0.93	46.99±1.31	48.81±1.34

Parti: Particle size and entrapment efficiency are recorded as mean±standard deviation, where n=3, and cumulative % drug release data are recorded as mean±standard deviation, where n=3, PLGA-PEG-HA: Poly (lactic-co-glycolic acid)-polyethylene glycol hyaluronic acid

**Table 5:** ANOVA suggested statistical model of etoposide-loaded PLGA-PEG-HA nanoparticles

Responses	Model	Sequential P-value	Lack of Fit P-value	Adjusted R <sup>2</sup> value	Predicted R <sup>2</sup> Value
Average particle size (R1)	Quadratic	0.0224	0.1140	0.7850	-0.1466
Polydispersity index (R2)	Quadratic	0.0142	0.1519	0.7657	-0.2191
Zeta potential (R3)	Quadratic	0.2241	0.6220	0.4653	-0.8025
Entrapment Efficiency (R4)	Quadratic	0.0202	0.4909	0.8458	0.3934
Cumulative % drug release in 5 min (R5)	Quadratic	0.2455	0.2305	0.1855	-3.0131
Cumulative % drug release in 15 min (R6)	Quadratic	0.1307	0.0302	0.2321	-3.3121
Cumulative % drug release in 30 min (R7)	Quadratic	0.0890	0.0466	0.3485	-2.6277
Cumulative % drug release in 60 min (R8)	Quadratic	0.2529	0.0173	0.0643	-4.2938
Cumulative % drug release in 120 min (R9)	Quadratic	0.0210	0.0435	0.7485	-0.4011
Cumulative % drug release in 240 min (R10)	Quadratic	0.0379	0.0873	0.7360	-0.4318
Cumulative % drug release in 360 min (R11)	Quadratic	0.0102	0.2878	0.8371	0.2310

PLGA-PEG-HA: Poly (lactic-co-glycolic acid)-polyethylene glycol hyaluronic acid

**Table 6:** Predicted value and the experimentally observed value of variables of the optimized batch of etoposide-loaded PLGA-PEG-HA nanoparticles

Components	Quantity		
A: Concentration of Drug	10 mg		
B: Concentration of PLGA-PEG-HA	98.395 mg		
C: Concentration of surfactant	0.348%		
Evaluation parameter	Predicted value	Practically observed value	Relative error (%)
Particle size (nm)	292.77	283.30±1.53.	3.21
Polydispersity index	0.50	0.57	14.51
Zeta potential	-7.98	-8.75	9.69
Entrapment efficiency	52.11	53.21	2.11
Cumulative % drug release in 5 min	9.64	10.69±1.07	10.92
Cumulative % drug release in 15 min	23.33	24.36±0.94	4.46
Cumulative % drug release in 30 min	27.22	26.22±0.86	3.67
Cumulative % drug release in 60 min	35.50	36.43±1.98	2.59
Cumulative % drug release in 120 min	46.57	47.77±1.48	2.55
Cumulative % drug release in 240 min	53.46	55.80±1.42	4.36
Cumulative % drug release in 360 min	61.26	63.33±1.16	3.36

Particle size is recorded as mean±standard deviation, where n=3, Cumulative % drug release data are recorded as mean±standard deviation, where n=3, PLGA-PEG-HA: Poly (lactic-co-glycolic acid)-polyethylene glycol hyaluronic acid

**Table 7:** Drug release kinetic model fitting of the release profile data of optimized batch of etoposide-loaded PLGA-PEG-HA nanoparticles

S. No.	Kinetic models	Mathematical equation	K value (mol/min)	R <sup>2</sup>
1.	Zero order model	$Q_0 - Q_t = k_0 t$	$1.85 \times 10^{-1}$	0.9370
2.	First order model	$\log Q = \log Q_0 - kt/2.303$	$1.30 \times 10^{-3}$	0.9387
3.	Korsmeyer-Peppas model	$\log (Q_0 - Q_t) = \log k - n \log t$	$6.925 \times 10^1$	0.9714
4.	Higuchi model	$Q_0 - Q_t = kt^{1/2}$	$3.17 \times 10^0$	0.9080
5.	Hixon-Crowell model	$Q_0^{1/3} - Q_t^{1/3} = kt$	$3.20 \times 10^{-3}$	0.8967

PLGA-PEG-HA: Poly (lactic-co-glycolic acid)-polyethylene glycol hyaluronic acid

samples were weighed, sealed in an aluminum pan, and analyzed between 50°C and 350°C with a nitrogen flow of 20 mL/min. The thermograms are shown in Figure 29.

### X-ray diffraction (XRD) studies

XRD patterns of PLGA-PEG-HA copolymer, a physical mixture of PLGA-PEG-HA and etoposide (1:1), etoposide, and etoposide-loaded PLGA-PEG-HA nanoparticles were obtained using an X-ray diffractometer (Bruker D8 Advance) to investigate the polymorphic nature of the materials. Copper K-alpha radiation (wavelength 0.154 nm) was generated using a sealed tube and detected using fast-counting detectors with silicon strip technology (Bruker Lynx Eye) at an angle of  $2\theta$  in the range of 5°–60°. The XRD patterns are shown in Figure 30.

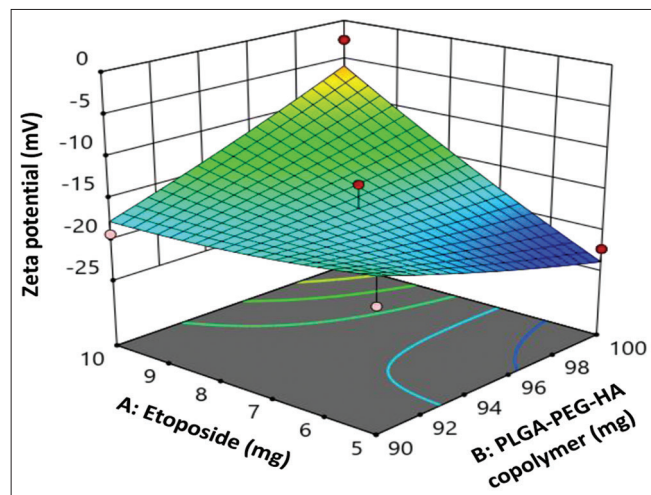


**Figure 6:** 3-D plot of the effect of etoposide and poly (lactic-co-glycolic acid)-polyethylene glycol hyaluronic acid copolymer on zeta potential

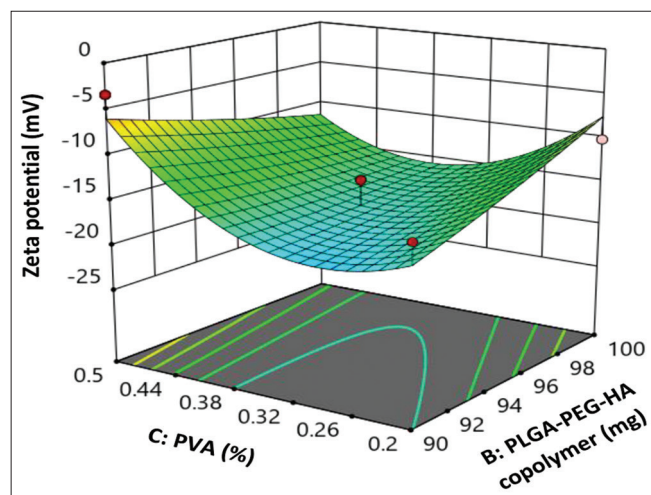


**Figure 7:** 3-D plot of the effect of polyvinyl alcohol and poly (lactic-co-glycolic acid)-polyethylene glycol hyaluronic acid copolymer on zeta potential

### *In vitro* release profile of the drug

The *in vitro* release profile of etoposide-loaded PLGA-PEG-HA nanoparticles were studied using phosphate buffer pH 7.4 comprising 0.1% w/v tween-80 as dissolving media. 100 mL of the phosphate buffer pH 7.4 comprising 0.1% w/v tween-80 was added to a stirred cell ultrafiltration apparatus along with 20 mg of etoposide-loaded PLGA-PEG-HA nanoparticles. At predefined intervals, 5 mL of the sample was withdrawn from the stirred cell under low pressure using a nitrogen flow and was replaced with 5 mL of fresh phosphate buffer with a pH of 7.4 containing 0.1% w/v tween-80.<sup>[21]</sup> The sample was examined using UV spectroscopy at 283 nm. The release data of the optimization batches and the optimized batch are recorded in Tables 4 and 6 and graphically shown in Figures 1 and 15. The comparison of software predicted and practically observed *in vitro* release profile is shown in Table 6 and the regression plot is represented in Figure 26.

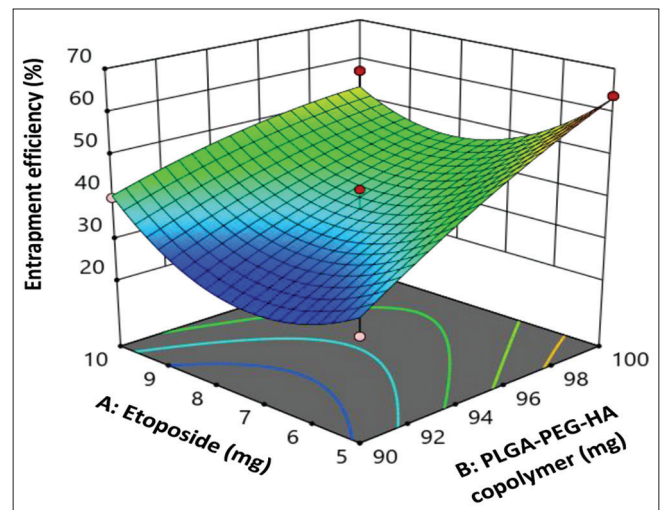


**Figure 8:** 3-D plot of the effect of poly (lactic-co-glycolic acid)-polyethylene glycol hyaluronic acid copolymer and etoposide on entrapment efficiency

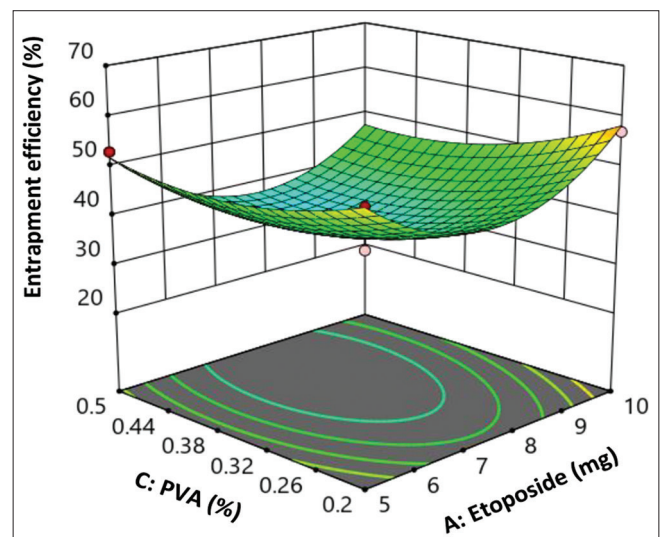


**Figure 9:** 3-D plot of the effect of polyvinyl alcohol and etoposide on entrapment efficiency



### Cytotoxicity analysis

The cytotoxicity of the synthesized nanoparticles was assessed on A549 cancer cells using an MTT assay.<sup>[22]</sup> MTT [(3-(4,5-dimethylthiazol-2-yl)-2,5-diphenyl tetrazolium bromide)] is a chemical that is converted into purple formazan crystals when it comes into contact with the mitochondria of living cells. The A549 cells were cultured in RPMI-1640 medium supplemented with 10% fetal bovine serum and antibiotics. In this assay, the synthesized nanoparticles were suspended in the culture medium and serially diluted in concentrations of 0.001 µg/mL, 0.01 µg/mL, 0.1 µg/mL, 1 µg/mL, and 10 µg/mL. Etoposide was separately dissolved in DMSO and serially diluted in the same concentrations of 0.001 µg/mL, 0.01 µg/mL, 0.1 µg/mL, 1 µg/mL, and 10 µg/mL with the culture medium. A549 cells were seeded in 96 wells of a microtiter plate with test samples (10 µL) of various concentrations and incubated for 4 days at 37°C with 5% CO<sub>2</sub>. The positive control was established with A549 cells in a culture medium containing DMSO. After incubation, the wells received MTT and were

**Table 8:** Cytotoxic effect of etoposide and etoposide-loaded PLGA-PEG-HA nanoparticles on A549 cell linings

Concentration (µg/mL)	% Mortality	
	Etoposide-loaded PLGA-PEG-HA nanoparticles	Etoposide
0.001	3.27	8.92
0.01	12.58	11.54
0.1	35.26	30.24
1	41.29	39.41
10	72.14	60.59

PLGA-PEG-HA: Poly (lactic-co-glycolic acid)-polyethylene glycol hyaluronic acid

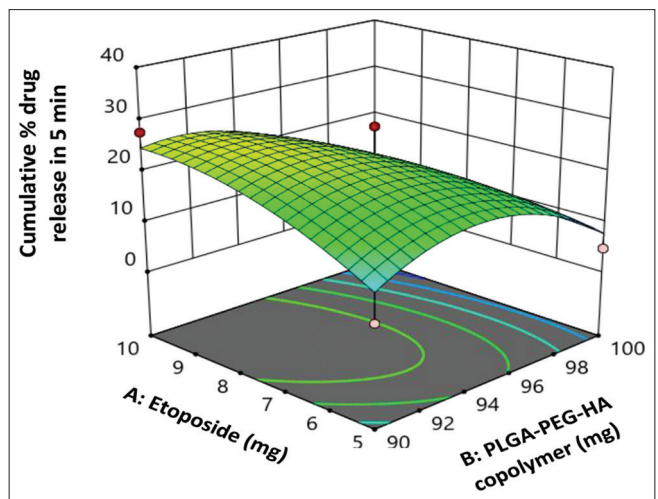


**Figure 10:** 3-D plot of the effect of etoposide and poly (lactic-co-glycolic acid)-polyethylene glycol hyaluronic acid copolymer on cumulative % drug release in 5 min

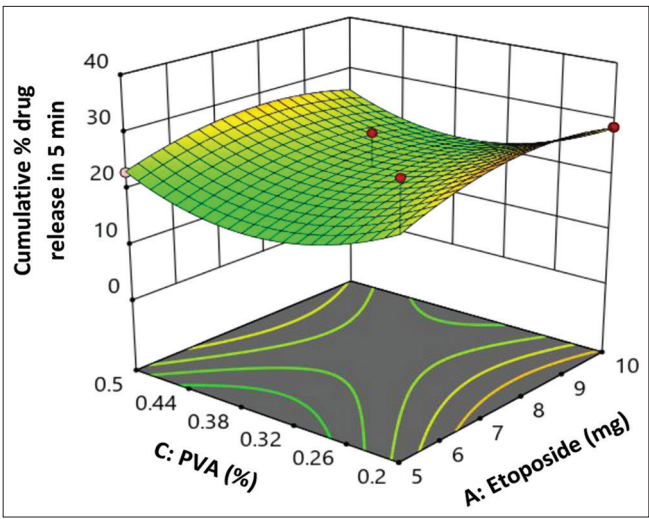


**Figure 11:** 3-D plot of the effect of etoposide and polyvinyl alcohol on cumulative % drug release in 5 min

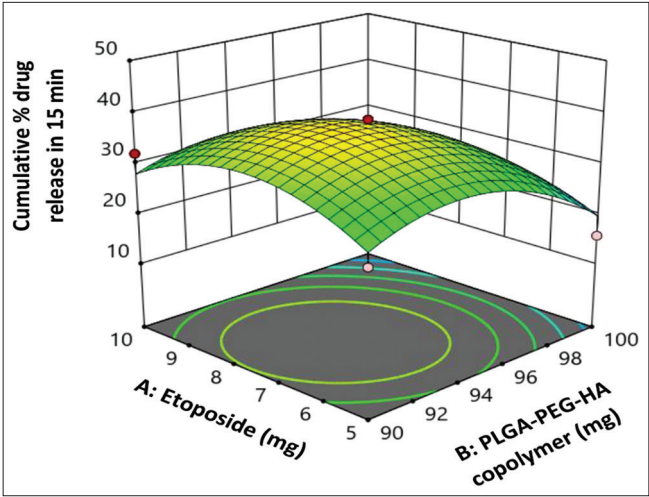


**Figure 12:** 3-D plot of the effect of etoposide and poly (lactic-co-glycolic acid)-polyethylene glycol hyaluronic acid copolymer on cumulative % drug release in 15 min

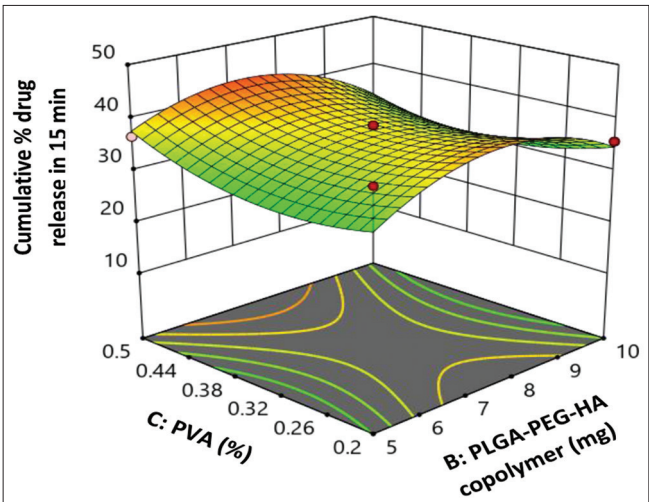


**Figure 13:** 3-D plot of the effect of etoposide and polyvinyl alcohol on cumulative % drug release in 15 min

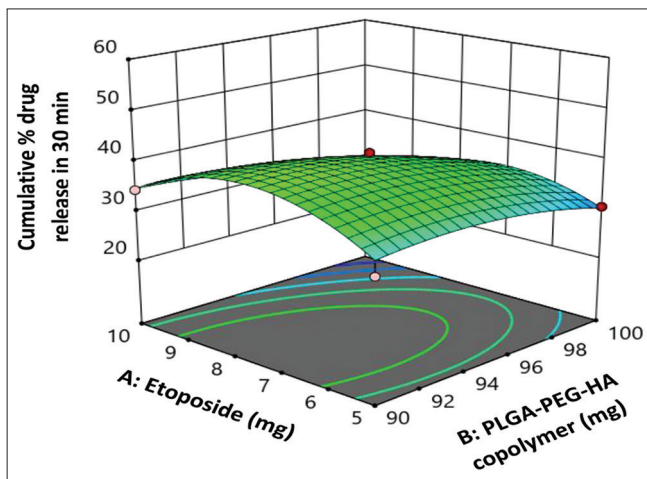


**Figure 14:** 3-D plot of the effect of etoposide and poly (lactic-co-glycolic acid)-polyethylene glycol hyaluronic acid copolymer on cumulative % drug release in 30 min

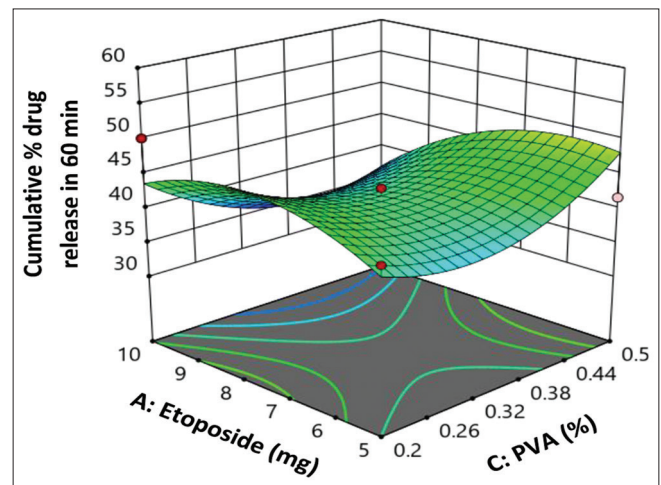


**Figure 17:** 3-D plot of the effect of etoposide and polyvinyl alcohol on cumulative % drug release in 60 min

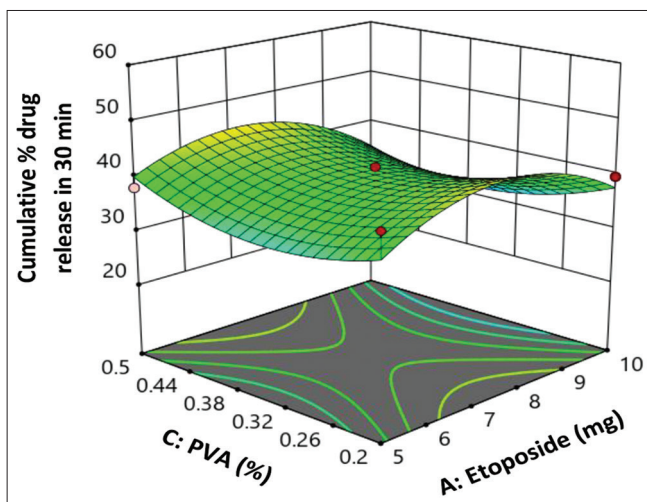


**Figure 15:** 3-D plot of the effect of etoposide and polyvinyl alcohol on cumulative % drug release in 30 min

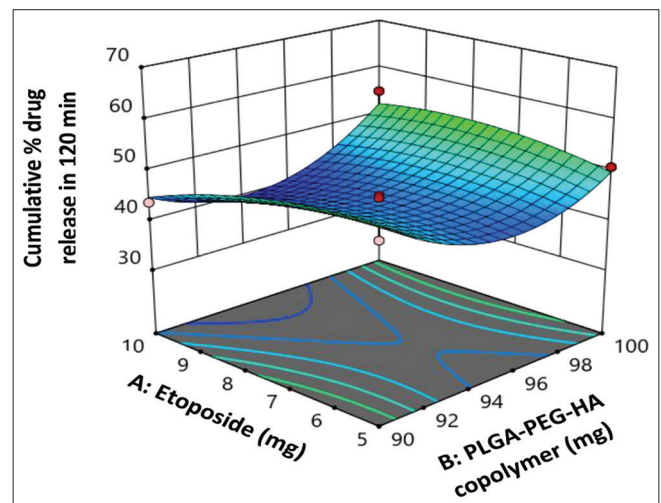


**Figure 18:** 3-D plot of the effect of etoposide and poly (lactic-co-glycolic acid)-polyethylene glycol hyaluronic acid copolymer on cumulative % drug release in 120 min

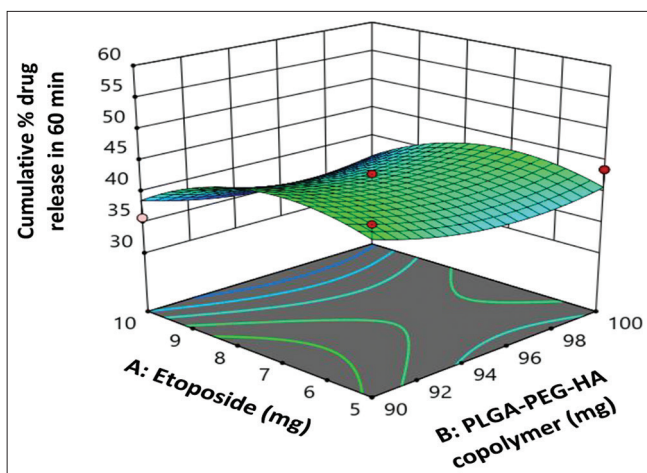


**Figure 16:** 3-D plot of the effect of etoposide and poly (lactic-co-glycolic acid)-polyethylene glycol hyaluronic acid copolymer on cumulative % drug release in 60 min

further incubated for 4 h to allow the formation of formazan crystals. The formazan crystals produced were dissolved in DMSO and read at 550 nm. The activity is recorded in Table 8.

## RESULTS AND DISCUSSION

### Optimization of etoposide-loaded PLGA-PEG-HA nanoparticles

The optimization of etoposide-loaded PLGA-PEG-HA nanoparticles was performed and independent variables, that is, etoposide (A), PLGA-PEG-HA copolymer (B), and PVA (C) were optimized. The limits of PLGA-PEG-HA copolymer (90–100 mg), etoposide (5–10 mg), and PVA (0.2–0.5%), respectively, were set in Design Expert® software and the particle size (R1), PDI (R2), zeta potential (R3), entrapment

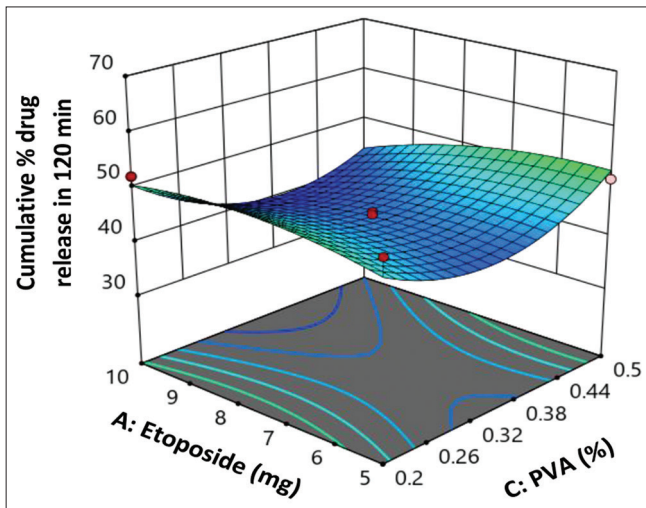


**Figure 19:** 3-D plot of the effect of etoposide and polyvinyl alcohol on cumulative % drug release in 120 min

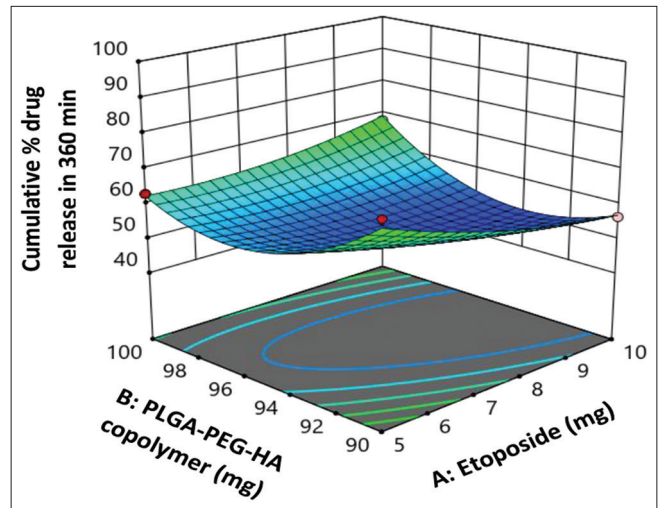


**Figure 22:** 3-D plot of the effect of etoposide and poly (lactic-co-glycolic acid)-polyethylene glycol hyaluronic acid copolymer on cumulative % drug release in 360 min

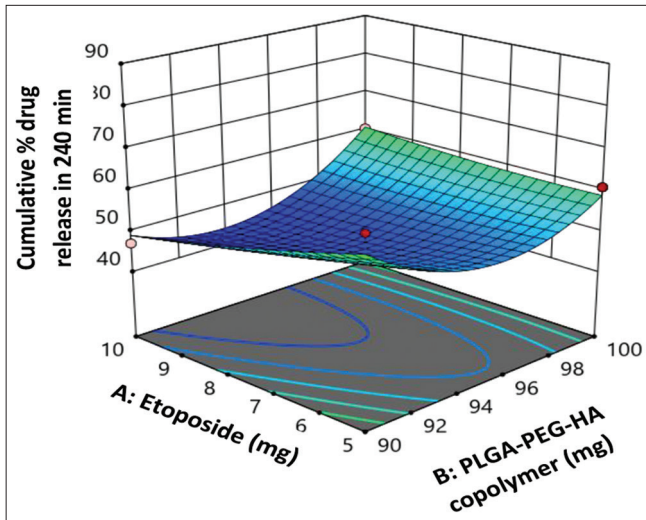


**Figure 20:** 3-D plot of the effect of etoposide and poly (lactic-co-glycolic acid)-polyethylene glycol hyaluronic acid copolymer on cumulative % drug release in 240 min

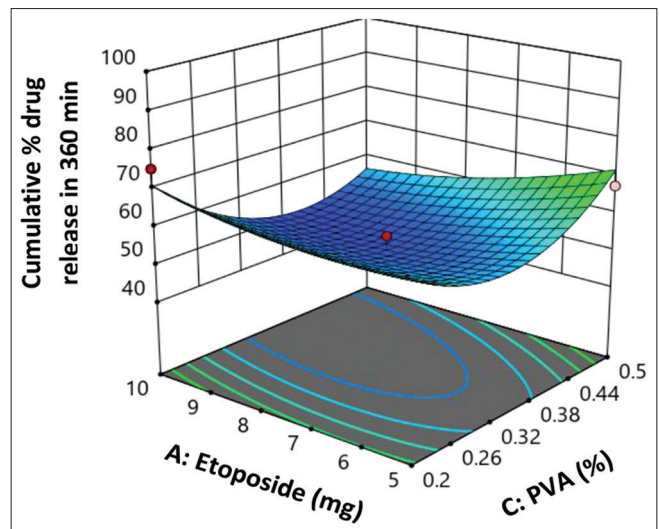


**Figure 23:** 3-D plot of the effect of etoposide and polyvinyl alcohol on cumulative % drug release in 360 min

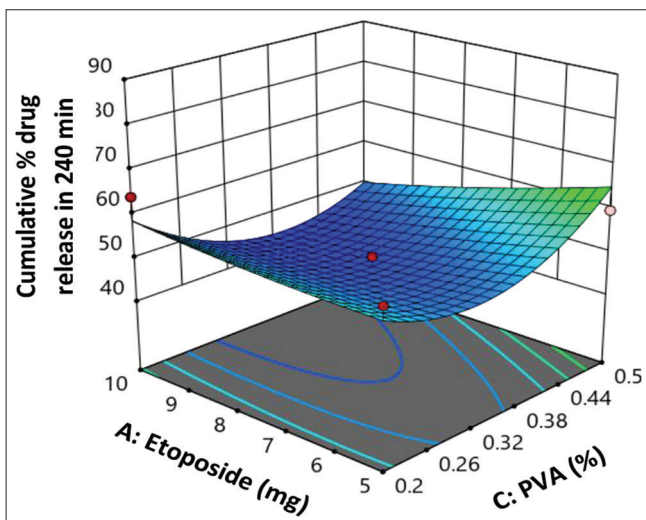


**Figure 21:** 3-D plot of the effect of etoposide and polyvinyl alcohol on cumulative % drug release in 240 min

efficiency (R4), and cumulative % drug release at different time points (R5-R11) of prepared etoposide-loaded PLGA-PEG-HA nanoparticles were set as response variables and the effect of the concentration of etoposide, PLGA-PEG-HA copolymer, and PVA on them were studied. The regression equations are recorded in Table 3, data is recorded in Table 4 and the statistical summary is recorded in Table 5. The optimal set of parameters that result in the desired characteristics of the nanoparticles was determined. The desired responses of etoposide-loaded PLGA-PEG-HA nanoparticles were particle size, zeta potential, PDI to be minimum, maximum entrapment efficiency, and sustained drug release pattern. The particle size of the nanoparticles is affected by the concentration of independent variables. The 3-D response curve in Figures 2 and 3 shows that the average particle size increases as the concentration of the polymer and drug increases as a result of the increase in the viscosity of the dispersed phase

in an emulsion that leads to difficulty in the ability to apply shear during sonication, resulting in the formation of larger globules and decreases as the concentration of surfactant increases due to the inability of coalescence of emulsion

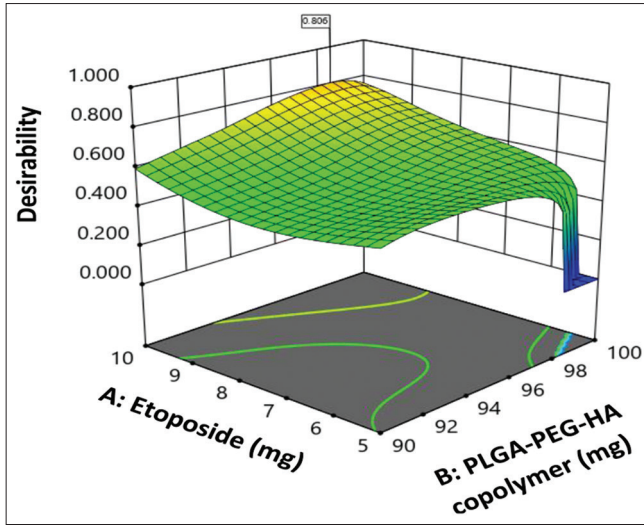


**Figure 24:** 3-D response surface plot of the desirability of etoposide-loaded poly (lactic-co-glycolic acid)-polyethylene glycol hyaluronic acid nanoparticles

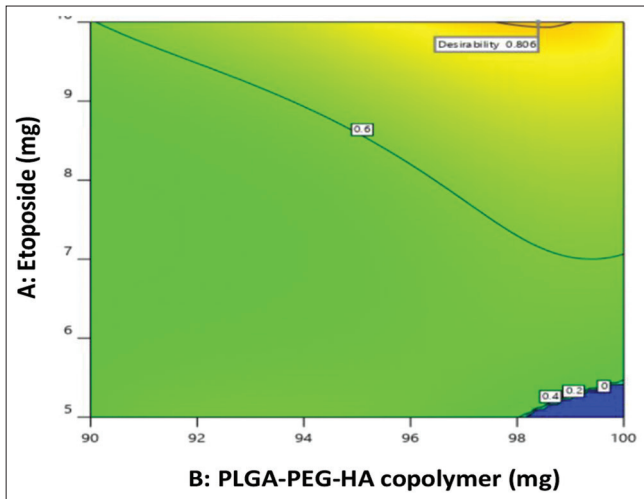


**Figure 25:** Contour plot of the desirability of etoposide-loaded poly (lactic-co-glycolic acid)-polyethylene glycol hyaluronic acid nanoparticles

droplets.<sup>[23,24]</sup> Minimum PDI signifies mono dispersity which is an important attribute for sustained release. The 3-D response curve in Figures 4 and 5 shows that the PDI decreases as the concentration of the surfactant increases. Zeta potential is a measure of charge, same charges repelling each other. PLGA-PEG-HA copolymer and PVA solution are negatively charged. The 3-D response curve in Figures 6 and 7 shows that the zeta potential decreases as the concentration of polymer and surfactant is increased and increases as the drug concentration increases.<sup>[25]</sup> The 3-D response curve in Figures 8 and 9 shows that the drug entrapment efficiency increases with an increase in PLGA-PEG-HA polymer, as the viscosity of the solution may also increase, which aids in trapping the drug molecules within the polymer and decreases with an increase in etoposide and PVA concentration, respectively, as the drug is present more in the aqueous phase and interacts less with PLGA-PEG-HA copolymer.<sup>[25]</sup>

Targeted drug delivery systems are designed to deliver a maximum amount of drug to the targeted site and a minimal amount initially, to maximize the therapeutic effect and minimize side effects. The release of etoposide from PLGA-PEG-HA nanoparticles decreases as the concentration of the copolymer increases, due to the physical entrapment of the drug within the nanoparticle matrix and the protective coating formed by the copolymer.<sup>[26]</sup> However, increasing the concentration of etoposide may disrupt the structure of the nanoparticle matrix and lead to a more rapid release of the drug. It is found that the concentration of PLGA-PEG-HA and etoposide affects the dependent responses (R5–R11), that is, cumulative % drug release in 5 min, 15 min, 30 min, 60 min, 120 min, 240 min, and 360 min, respectively. The 3-D response surface curve in Figures 10-23, shows that increasing the polymer concentration decreases the drug release whereas increasing the drug concentration increases the drug release from nanoparticles. The sustained action of the nanoparticles is solely attributed to the concentration of the polymer present.

### Prediction of optimized formulation of etoposide-loaded PLGA-PEG-HA nanoparticles

The design expert software analyzed the results of the optimization batches and predicted the independent

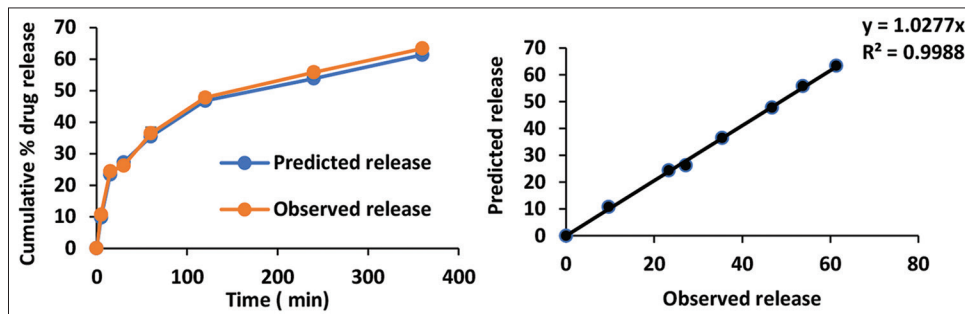


**Figure 26:** Predicted and experimentally observed in-vitro release profile of drug and regression plot of optimized formulation of etoposide-loaded poly (lactic-co-glycolic acid)-polyethylene glycol hyaluronic acid nanoparticles

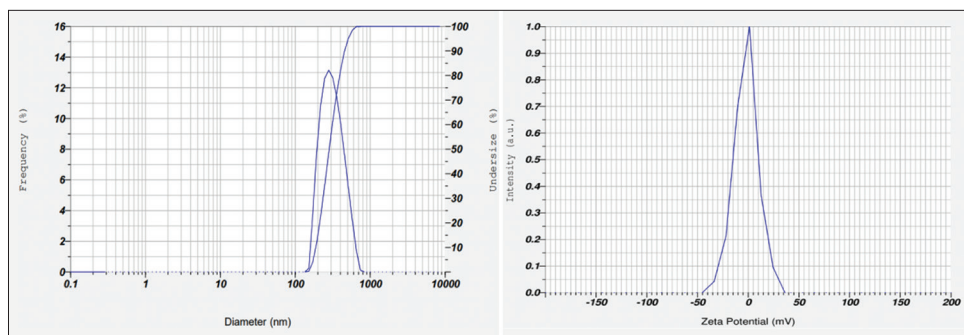


**Figure 27:** Particle size distribution and zeta potential of etoposide-loaded poly (lactic-co-glycolic acid)-polyethylene glycol hyaluronic acid nanoparticle

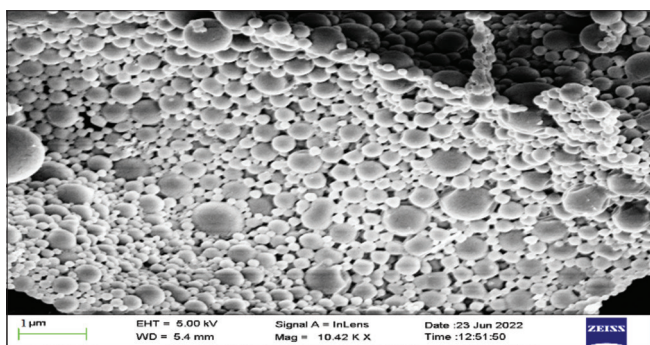


**Figure 28:** SEM image of etoposide-loaded poly (lactic-co-glycolic acid)-polyethylene glycol hyaluronic acid nanoparticles

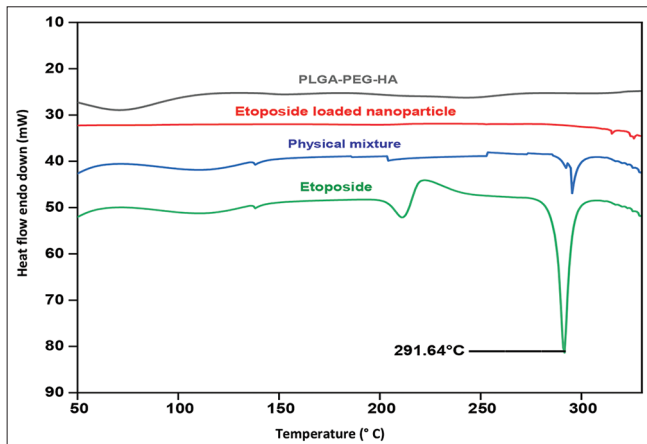


**Figure 29:** Thermogram of etoposide, poly (lactic-co-glycolic acid)-polyethylene glycol hyaluronic acid (PLGA-PEG-HA), etoposide-loaded PLGA-PEG-HA nanoparticles, physical mixture of etoposide and PLGA-PEG-HA

and dependent variables of the optimized batch with a desirability of 0.806 as shown in Figures 24 and 25, which was composed of etoposide (10.00 mg), PLGA-PEG-HA copolymer (98.39 mg), and PVA (0.34%) that resulted in a desirable outcome, as measured by the dependent variables, that is, average particle size, PDI, zeta potential, entrapment efficiency, and cumulative % drug release at 5, 15, 30, 60, 120, 240, and 360 min. The practically observed results were compared to the software-predicted results and are recorded

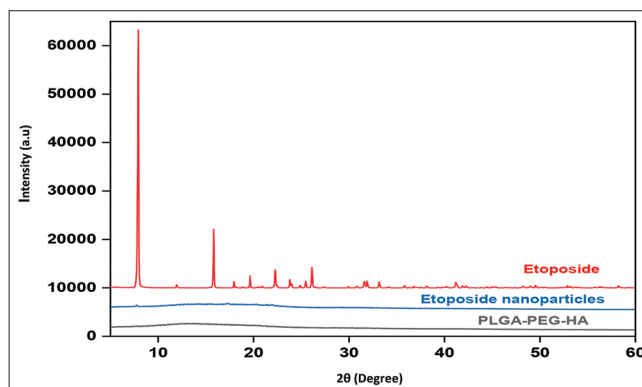


**Figure 30:** XRD pattern of etoposide, etoposide-loaded poly (lactic-co-glycolic acid)-polyethylene glycol hyaluronic acid (PLGA-PEG-HA) nanoparticles, PLGA-PEG-HA

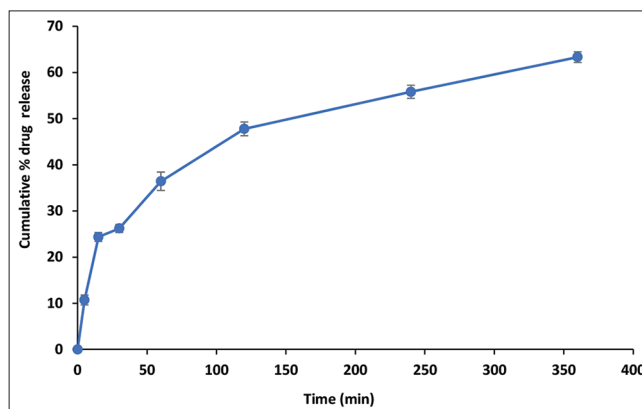


**Figure 31:** *In vitro* release profile of optimized batch of etoposide-loaded poly (lactic-co-glycolic acid)-polyethylene glycol hyaluronic acid nanoparticles

in Table 6. The regression coefficient ( $R^2$ ) calculated was 0.9997 and the correlation coefficient calculated was 0.9576 which were close to 1.

### Particle size, zeta potential, and SEM

The observed average particle size of the optimized etoposide-loaded PLGA-PEG-HA nanoparticles was 283.30 nm with PDI 0.57 and zeta potential  $-8.75$  mV, as shown in Figure 27. Particle size in the nano-range facilitates the fast release of

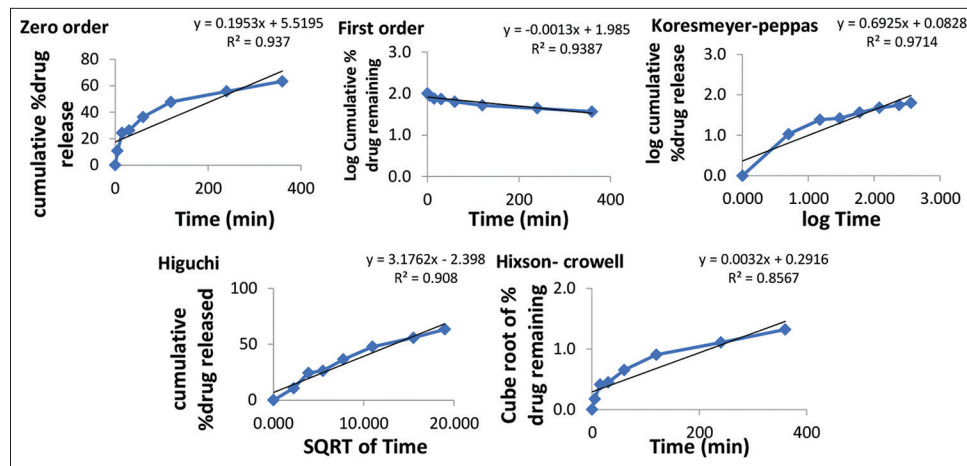


**Figure 32:** Kinetic modeling of etoposide-loaded poly (lactic-co-glycolic acid)-polyethylene glycol hyaluronic acid nanoparticles

drug.<sup>[27]</sup> Negative zeta potential shows that nanoparticles are stable and are less toxic to the cell wall.<sup>[28]</sup> The SEM analysis demonstrates that particles were spherical, smooth, and not aggregated as shown in Figure 28.

### DSC and XRD analysis

The polymorphic form of materials is analyzed using DCS and XRD. The DSC thermograms of etoposide, PLGA-PEG-HA, physical mixture, and etoposide-loaded PLGA-PEG-HA nanoparticles are shown in Figure 29. Etoposide shows an endothermic peak at 291.64°C that confirms its crystalline nature. PLGA-PEG-HA shows no sharp peak and hence confirms its amorphous nature. The physical mixture shows the endothermic peak of etoposide. The thermogram of etoposide-loaded PLGA-PEG-HA nanoparticles shows no endothermic peak of etoposide, indicating that the entrapped drug was in an amorphous state inside the nanoparticles.<sup>[29]</sup>

XRD patterns of etoposide, PLGA-PEG-HA, and etoposide-loaded PLGA-PEG-HA nanoparticles are shown in Figure 30. Etoposide shows sharp peaks at 7.93, 15.82, 22.27, and 26.09  $\theta$  due to its crystalline nature. PLGA-PEG-HA shows no sharp peak in the XRD pattern showing its amorphous nature. Etoposide-loaded PLGA-PEG-HA nanoparticles show no distinct crystalline peak of etoposide confirming the amorphous nature of entrapped drug into nanoparticles.<sup>[30]</sup>

### In vitro drug release profile of the drug

The release profile of the formulated optimized batch was carried out in phosphate buffer 7.4 consisting of 0.1% w/v tween 80 as dissolution medium and data was recorded. The cumulative % drug release in 5 min ranges from 4.72% to 34.06% and in 360 min ranges from 51.15% to 90.47% as recorded in Table 4 and graphically shown in Figure 1. The 3-D response surface plots of optimization batches are represented in Figures 11-23. The *in vitro* release of optimized

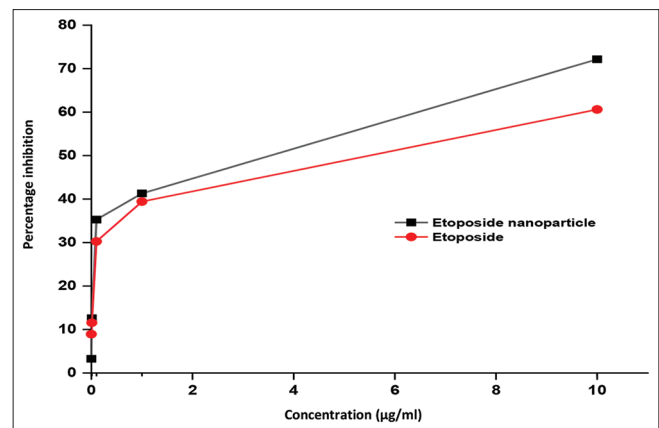


**Figure 33:** Effect of etoposide-loaded poly (lactic-co-glycolic acid)-polyethylene glycol hyaluronic acid nanoparticles and etoposide on inhibition of cancer cells

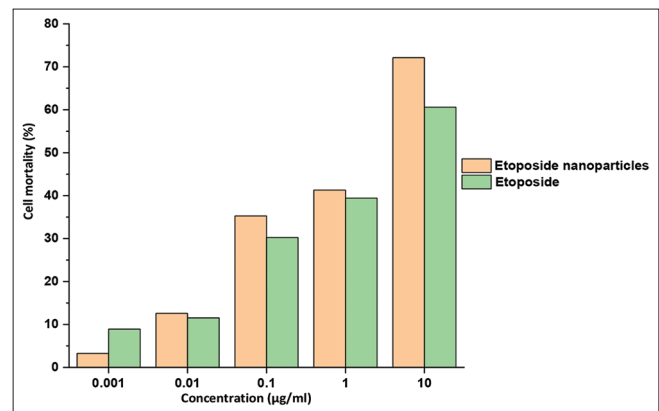


**Figure 34:** Effect of etoposide-loaded poly (lactic-co-glycolic acid)-polyethylene glycol hyaluronic acid nanoparticles and etoposide on mortality of A549 cell linings

PLGA-PEG-HA nanoparticles showed a release of 63.33% as recorded in Table 6 and represented in Figure 31. There is an initial burst release of the drug followed by sustained release due to PLGA-PEG-HA copolymer. The initial rapid release of the drug is due to the drug that is on the surface of the nanoparticle, which is released quickly when the nanoparticle

is exposed to the dissolution medium.<sup>[31]</sup> The sustained release is usually to the drug that is contained within the nanoparticle matrix and is released at a slower rate.<sup>[32]</sup>

### Kinetic modeling of drug release

The drug release profile data for the optimized batch of etoposide-loaded PLGA-PEG-HA nanoparticles were analyzed using various mathematical models, including the zero-order model, first-order model, Higuchi model, Korsmeyer-Peppas model, and Hixson-Crowell model. The observations were recorded in Tables 6 and 7, showing that the Korsmeyer-Peppas model provided the accurate fit for the data, with an  $R^2$  value of 0.9714. This is shown in Figure 32. The release exponent “n,” which represents the release rate, was found to be 0.5982, indicating that the drug release follows an anomalous, non-Fickian pattern in the Korsmeyer-Peppas model. The release of the drug by the nanoparticles takes place through erosion of the polymer matrix rather than through diffusion, which is typically observed in systems with a homogenous distribution of particles.<sup>[33,34]</sup>

### Cytotoxicity study

The cytotoxic study of etoposide, etoposide-loaded PLGA-PEG-HA nanoparticles, and placebo of PLGA-PEG-HA nanoparticles was examined on the A549 lung cell line. Inhibition of cell growth by etoposide and etoposide-loaded nanoparticle was proportional to drug dose as shown in Figures 33 and 34. It was observed that etoposide-loaded PLGA-PEG-HA nanoparticles show higher toxicity than etoposide. The higher toxicity of etoposide-loaded PLGA-PEG-HA nanoparticles is attributed to their uptake by CD44 receptors on the A549 cell lines.

## CONCLUSION

The most prevalent form of lung cancer is SCLC, which is primarily caused by smoking. Conventional formulations of drugs used to treat this condition often result in significant side effects due to a lack of site-specific targeting. In this study, PLGA-PEG-HA nanoparticles were synthesized as a drug delivery system for etoposide to lung cancer cells in a sustained manner, and the BBD of response surface methodology was used to optimize the formulations. The optimized batch exhibited an average particle size of 283.30 nm, a PDI of 0.57, an zeta potential of  $-8.7$  mV, and an entrapment efficiency of 53.21%. SEM, DSC, and XRD analyses demonstrated that the nanoparticles were spherical, non-porous, and effectively encapsulated the drug. The MTT assay on A549 cell lines showed that etoposide nanoparticles were selectively taken up by lung cancer cells due to their strong affinity for CD44 receptors through HA. The conventional etoposide formulations available lack site-specific action and have higher side effects associated with the

drug. PLGA-PEG-HA nanoparticles have the potential to be a promising delivery system for cancer therapy in a site-specific manner and reduce the side effects associated with the drug by reducing its exposure to normal non-cancerous sites.

## ACKNOWLEDGMENT

The authors acknowledges AICTE, New Delhi, and MPCST, Bhopal for providing a grant for research facilities, UGC-DAE for XRD analysis, IIT, Indore for SEM analysis, VNS college of pharmacy, Bhopal for particle size analysis and zeta potential analysis, and M/s Zydus Research Center, Ahmedabad for providing a drug sample.

## REFERENCES

1. Siddiqui F, Vaqar S, Siddiqui AH. Lung Cancer. Treasure Island (FL): StatPearls Publishing; 2022.
2. Society AC. Cancer Facts and Figures 2014. United States: American Cancer Society; 2014.
3. Vallieres E, Shepherd FA, Crowley J, Van Houtte P, Postmus PE, Carney D, *et al.* The IASLC Lung cancer staging project: Proposals regarding the relevance of TNM in the pathologic staging of small cell lung cancer in the forthcoming (seventh) edition of the TNM classification for lung cancer. *J Thorac Oncol* 2009;4:1049-59.
4. Henwood JM, Brogden RN. Etoposide. A review of its pharmacodynamic and pharmacokinetic properties, and therapeutic potential in combination chemotherapy of cancer. *Drugs* 1990;39:438-90.
5. Baldwin E, Osheroff N. Etoposide, topoisomerase II and cancer. *Curr Med Chem Anticancer Agents* 2005;5:363-72.
6. Smith MA, Rubinstein L, Anderson JR, Arthur D, Catalano PJ, Freidlin B, *et al.* Secondary leukemia or myelodysplastic syndrome after treatment with epipodophyllotoxins. *J Clin Oncol* 1999;17:569-77.
7. Bhatia S. Nanoparticles types, classification, characterization, fabrication methods and drug delivery applications. In: *Natural Polymer Drug Delivery Systems*. Germany: Springer; 2016. p. 33-93.
8. Attia MF, Anton N, Wallyn J, Omran Z, Vandamme TF. An overview of active and passive targeting strategies to improve the nanocarriers efficiency to tumour sites. *J Pharm Pharmacol* 2019;71:1185-98.
9. De Jong WH, Borm PJ. Drug delivery and nanoparticles: Applications and hazards. *Int J Nanomedicine* 2008;3:133-49.
10. Alam N, Khare V, Dubey R, Saneja A, Kushwaha M, Singh G, *et al.* Biodegradable polymeric system for cisplatin delivery: Development, *in vitro* characterization and investigation of toxicity profile. *Mater Sci Eng C Mater Biol Appl* 2014;38:85-93.
11. Dinauer N, Balthasar S, Weber C, Kreuter J,

- Langer K, von Briesen H. Selective targeting of antibody-conjugated nanoparticles to leukemic cells and primary T-lymphocytes. *Biomaterials* 2005;26:5898-906.
12. Mattheolabakis G, Rigas B, Constantinides PP. Nanodelivery strategies in cancer chemotherapy: Biological rationale and pharmaceutical perspectives. *Nanomedicine* 2012;7:1577-90.
  13. Resnick NM, Clarke MR, Siegfried JM, Landreneau R, Asman DC, Ge L, *et al.* Expression of the cell adhesion molecule CD44 in human lung tumors and cell lines. *Mol Diagn* 1998;3:93-103.
  14. Hiscox S, Baruah B, Smith C, Bellerby R, Goddard L, Jordan N, *et al.* Overexpression of CD44 accompanies acquired tamoxifen resistance in MCF7 cells and augments their sensitivity to the stromal factors, heregulin and hyaluronan. *BMC Cancer* 2012;12:458.
  15. Misra S, Heldin P, Hascall VC, Karamanos NK, Skandalis SS, Markwald RR, *et al.* Hyaluronan-CD44 interactions as potential targets for cancer therapy. *FEBS J* 2011;278:1429-43.
  16. Paswan SK, Saini TR, Jahan S, Ganesh N. Designing and formulation optimization of hyaluronic acid conjugated PLGA nanoparticles of tamoxifen for tumor targeting. *Pharm Nanotechnol* 2021;9:217-35.
  17. Elsewedy HS, Al Dhubiab BE, Mahdy MA, Elnahas HM. Development, optimization, and evaluation of PEGylated brucine-loaded PLGA nanoparticles. *Drug Deliv* 2020;27:1134-46.
  18. Kocbek P, Obermajer N, Cegnar M, Kos J, Kristl J. Targeting cancer cells using PLGA nanoparticles surface modified with monoclonal antibody. *J Control Release* 2007;120:18-26.
  19. Pecora R. Dynamic light scattering measurement of nanometer particles in liquids. *J Nanoparticle Res* 2000;2:123-31.
  20. Tucker IM, Corbett JC, Fatkin J, Jack RO, Kaszuba M, MacCreath B, *et al.* Laser Doppler Electrophoresis applied to colloids and surfaces. *Curr Opin Colloid Interface Sci* 2015;20:215-26.
  21. Paswan SK, Saini T. Comparative evaluation of *in vitro* drug release methods employed for nanoparticle drug release studies. *Clin Trials J* 2021;14:17.
  22. Kanintronkul Y, Worayuthakarn R, Thasana N, Winayanuwattikun P, Pattanapanyasat K, Surarit R, *et al.* Overcoming multidrug resistance in human lung cancer with novel benzo [a] quinolizin-4-ones. *Anticancer Res* 2011;31:921-7.
  23. Khan R, Inam MA, Khan S, Jiménez AN, Park DR, Yeom IT. The influence of ionic and nonionic surfactants on the colloidal stability and removal of CuO nanoparticles from water by chemical coagulation. *Int J Environ Res Public Health* 2019;16:1260.
  24. Mainardes RM, Evangelista RC. PLGA nanoparticles containing praziquantel: Effect of formulation variables on size distribution. *Int J Pharm* 2005;290:137-44.
  25. Song X, Zhao Y, Hou S, Xu F, Zhao R, He J, *et al.* Dual agents loaded PLGA nanoparticles: Systematic study of particle size and drug entrapment efficiency. *Eur J Pharm Biopharm* 2008;69:445-53.
  26. Averineni RK, Shavi GV, Gurram AK, Deshpande PB, Arumugam K, Maliyakkal N, *et al.* PLGA 50: 50 nanoparticles of paclitaxel: Development, *in vitro* anti-tumor activity in BT-549 cells and *in vivo* evaluation. *Bull Mater Sci* 2012;35:319-26.
  27. Rizvi SA, Saleh AM. Applications of nanoparticle systems in drug delivery technology. *Saudi Pharm J* 2018;26:64-70.
  28. Clogston JD, Patri AK. Zeta potential measurement. In: *Characterization of Nanoparticles Intended for Drug Delivery*. Germany: Springer; 2011. p. 63-70.
  29. Arora D, Kumar A, Gupta P, Chashoo G, Jaglan S. Preparation, characterization and cytotoxic evaluation of bovine serum albumin nanoparticles encapsulating 5-methylmellein: A secondary metabolite isolated from *Xylaria psidii*. *Bioorg Med Chem Lett*. 2017;27:5126-30.
  30. Zhang JY, He B, Qu W, Cui Z, Wang YB, Zhang H, *et al.* Preparation of the albumin nanoparticle system loaded with both paclitaxel and sorafenib and its evaluation *in vitro* and *in vivo*. *J Microencapsul* 2011;28:528-36.
  31. Mainardes RM, Evangelista RC. Praziquantel-loaded PLGA nanoparticles: Preparation and characterization. *J Microencapsul* 2005;22:13-24.
  32. Corrigan OI, Li X. Quantifying drug release from PLGA nanoparticulates. *Eur J Pharm Sci* 2009;37:477-85.
  33. Korsmeyer RW, Gurny R, Doelker E, Buri P, Peppas NA. Mechanisms of solute release from porous hydrophilic polymers. *Int J Pharm* 1983;15:25-35.
  34. Scholes PD, Coombes AG, Illum L, Davis SS, Watts JF, Ustariz C, *et al.* Detection and determination of surface levels of poloxamer and PVA surfactant on biodegradable nanospheres using SSIMS and XPS. *J Control Release* 1999;59:261-78.

**Source of Support:** Nil. **Conflicts of Interest:** None declared.